Inhibition of the Cytolytic Protein Perforin Prevents Rejection of Transplanted Bone Marrow Stem Cells in Vivo

Julie A. Spicer,*[†,‡] Christian K. Miller,[†,‡] Patrick D. O'Connor,[†,‡] Jiney Jose,[†,‡] Anna C. Giddens,[†] Jagdish K. Jaiswal,[†,‡] Stephen M. F. Jamieson,[†,‡,§] Matthew R. Bull,[†,‡] William A. Denny,[†,‡] Hedieh Akhlaghi,[∥] Joseph A. Trapani,[∥,⊥] Geoff R. Hill,[#] Karshing Chang,[#] and Kate H. Gartlan[#]

[†]Auckland Cancer Society Research Centre, Faculty of Medical and Health Sciences, The University of Auckland, Private Bag 92019, Auckland 1142, New Zealand

[‡]Maurice Wilkins Centre for Molecular Biodiscovery, A New Zealand Centre for Research Excellence, Auckland 1010, New Zealand

[§]Department of Pharmacology and Clinical Pharmacology, Faculty of Medical and Health Sciences, The University of Auckland, Private Bag 92019, Auckland 1142, New Zealand

[∥]Cancer Immunology Program, Peter MacCallum Cancer Centre, 305 Grattan Street, Melbourne, Victoria 3000, Australia

[⊥]Sir Peter MacCallum Department of Oncology, The University of Melbourne, Parkville, Victoria 3052, Australia

[#]QIMR Berghofer Medical Research Institute, 300 Herston Road, Herston, Queensland 4006, Australia

S *Supporting Information*
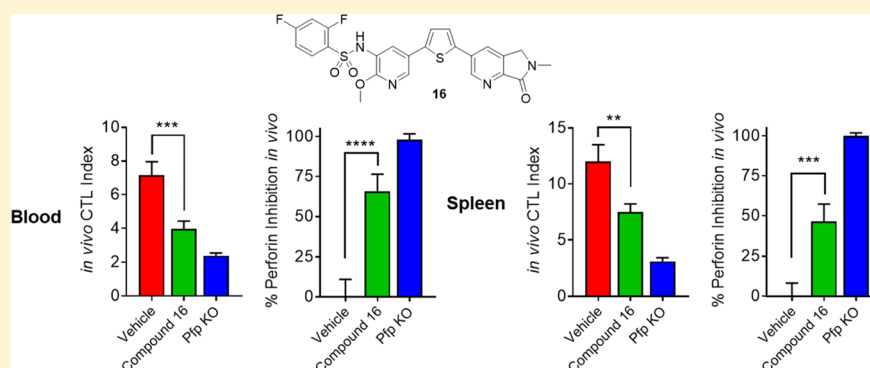
ABSTRACT: Perforin is a key effector protein in the vertebrate immune system and is secreted by cytotoxic T lymphocytes and natural killer cells to help eliminate virus-infected and transformed target cells. The ability to modulate perforin activity in vivo could be extremely useful, especially in the context of bone marrow stem cell transplantation where early rejection of immunologically mismatched grafts is driven by the recipient's natural killer cells, which overwhelmingly use perforin to kill their targets. Bone marrow stem cell transplantation is a potentially curative treatment for both malignant and nonmalignant disorders, but when the body recognizes the graft as foreign, it is rejected by this process, often with fatal consequences. Here we report optimization of a previously identified series of benzenesulfonamide-based perforin inhibitors for their physicochemical and pharmacokinetic properties, resulting in the identification of 16, the first reported small molecule able to prevent rejection of transplanted bone marrow stem cells in vivo by blocking perforin function.

INTRODUCTION

The pore-forming protein perforin[1] is an essential component of the vertebrate immune system and is found only in the secretory granules of cytotoxic T lymphocytes (CTLs) and natural killer (NK) cells. These "killer" cells eliminate virus-infected and tumor cells through a process known as the granule exocytosis pathway.[2] Upon stable conjugation of a CTL/NK cell and cognate target, a synaptic cleft is formed into which a mixture of perforin and granzymes (a group of serine proteases) is secreted.[3] The ability of perforin to disrupt the target cell membrane is critical for enabling entry of the proapoptotic granzymes into the cytoplasm where they trigger target cell death. Mutations that result in loss of perforin

expression or function result in fatal immune dysregulation, while partial loss has been associated with hematological or solid cancers.[3,4] Conversely, inappropriate perforin activity has been implicated in a variety of pathologies, including insulin-dependent diabetes, juvenile idiopathic arthritis, postviral myocarditis, and postviral acute liver failure[5−8] as well as therapy-induced conditions such as allograft rejection and graft versus host disease.[9−11]
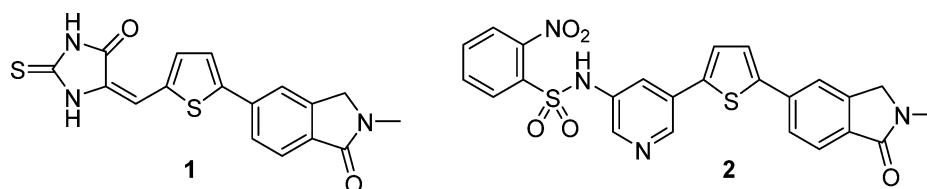
Figure 1. Previously published small molecule inhibitors of perforin.

Perforin is delivered into the immune synapse as soluble monomers, where upon exposure to calcium, it self-assembles into oligomeric pores of 10−20 nM internal diameter in the target cell membrane. This is necessarily a rapid process (<20 s) in order to overwhelm the membrane-repair response of the target cell and enable efficient diffusion of the granzymes into the cytosol.[12] Recently, this mechanism has been further elucidated, showing that the first step is the formation of loosely, but irreversibly, bound oligomers on the target cell membrane.[13] This is followed by insertion into the membrane which affords nucleation sites for further oligomer growth and assembly. The process is completed by the formation of perforin arc- and ring-shaped transmembrane pores that are then able to facilitate granzyme entry.

For several years we have been endeavoring to identify a small molecule inhibitor of perforin as a potential immuno-suppressive agent suitable for clinical use.[14−18] This is a novel approach as there are currently no treatments available that selectively block perforin-dependent cell death. Specifically, we are attempting to develop a therapy that will preserve transplanted bone marrow stem cells. Stem cell transplantation is a potentially curative treatment for hematological cancers as well as nonmalignant disorders such as bone marrow failure and inherited immunodeficiency disorders.[19] In the absence of a fully human leukocyte antigen (HLA)-matched donor, engraftment may rely on variably matched grafts of umbilical cord blood. HLA-half-matched-related (haploidentical) trans-plants from a patient's parents, siblings, or children are also increasingly being used,[20] resulting in an increased population of eligible patients and a predicted rapid rise in the number of stem cell transplants. However, this approach is also associated with a higher rate of graft rejection[21] by residual recipient cell populations that are able to survive and function after pretransplant radio- and chemotherapeutic conditioning regimens.[22] Since a second transplant is the only option for patients who experience graft failure, current research is focused on developing new therapeutic agents to improve engraftment and prevent immune-mediated graft rejection.[21]

Successful engraftment requires that the donor stem cells reach and gain access to the hematopoietic niche space where they can proliferate and restore bone marrow function.[23] Early rejection of mismatched grafts is driven by the recipient's NK cells which overwhelmingly use perforin to kill their targets and are capable of rejecting >85% of HLA-mismatched stem cell grafts within 48 h.[24−26] These cells are both radio-[27] and immune-suppressant-resistant,[24] and there are no clinical products that specifically delete NK cell function. The use of a perforin inhibitor to protect the transplanted stem cells in the critical period of 4−5 days immediately after transplantation would accelerate engraftment and minimize the use of traditional immunosuppressants which can be significantly toxic with multiple side effects. This approach is supported by genetic evidence demonstrating that while patients with total loss of perforin expression suffer from severe immune

dysfunction, those with a heterozygous perforin deficiency (50−75% perforin activity) show normal phenotypes, suggesting that a partial perforin blockade or short-term inhibition could be a permissible method of preventing stem cell rejection.[6,7] This therapy would not only address an urgent unmet need for patients who receive partially mismatched stem cell transplants but in the longer term also has the potential to improve outcomes in other indications (e.g., solid organ transplantation and autoimmune disorders).

To this end, we have previously identified several novel templates able to block the activity of both recombinant perforin and perforin produced by whole NK cells.[14−17] Our original lead structure (1; Figure 1) was based on a hit identified from a mass screen;[28] however this contained a potentially reactive Michael acceptor and showed variable toxicity toward the NK cells. We subsequently found that a pyridyl-linked benzenesulfonamide could act as a bioisosteric replacement for the problematic thiazolidinedione subunit, resulting in the identification of a new lead series.[16,17] A member of this series (2) was subsequently shown to dramatically enhance survival in a murine model of acute fulminant hepatitis.[18] In humans this is generally a fatal condition with no specific therapy available apart from a liver transplant. This is a key finding because it is the first demonstration of the in vivo activity of a small molecule perforin inhibitor in a disease that is driven by perforin-dependent cell-killing.[8,18]

In the current paper we report further optimization of the physicochemical and pharmacokinetic properties of these compounds, culminating in the identification of the first small molecule inhibitor capable of preventing rejection of transplanted bone marrow stem cells in vivo by blocking perforin function.

◼ RESULTS AND DISCUSSION

In our initial reports of benzenesulfonamide-based inhibitors of perforin[16,17] we described a large range of variations that were carried out on the lead molecule to establish a detailed structure−activity relationship. We determined that while substitution on the terminal benzene and central pyridine ring could be employed to modulate activity, the isoindoli-none, thiophene, pyridine, and sulfonamide units were close to optimal, meaning that the range of structures that could be accommodated while still retaining inhibitory activity was relatively narrow. In our current account we therefore focus on more subtle changes to the established template to improve physicochemical properties and in vivo pharmacokinetics to maximize potential for preventing rejection in a mouse model of bone marrow transplantation. In particular we sought to reduce lipophilicity (cLogP) and increase solubility. To do this, we implemented two approaches first by appending a "solubilizing" side chain to the isoindolinone nitrogen (compounds of Table 1) and second through the introduction of a nitrogen atom to the isoindolinone benzene ring, resulting

Table 1. Introduction of Solubilizing Side Chains

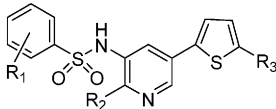| Cmpd	R₁	Inhibition of Jurkat Cell Lysis IC₅₀ (μM)[a]
3	⌣⌣OH	>20
4	morpholine	17.0
5	diol (OH, OH)	14.2
6	N(CH₃)₂	>20
7	pyrrolidine	>20
8	piperidine	>20
9	N-methylpiperazine	>20

[a]Testing was carried out over a range of concentrations, with the IC₅₀ being equal to the concentration at which 50% inhibition of the lysis of Jurkat cells by purified recombinant perforin was observed, as measured by ^{51}Cr release. Values are the average of at least three independent IC₅₀ determinations.

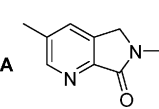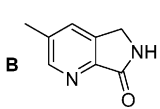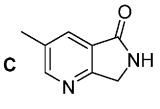in a series of 5,6-dihydro-7H-pyrrolo[3,4-b]pyridin-7-ones (compounds of Table 2).

Synthesis of the Target Compounds. The key iodides of Scheme 1 (18−24) were prepared as reported previously, through reaction of N-substituted-iodoisoindolinones[14] with 2-thiopheneboronic acid under Suzuki conditions, followed by iodination at the 2-position of the thiophene with N-iodosuccinimide.[16] Iodides 18 and 19 were coupled with BOC-5-bromo-3-aminopyridine to give 25 and 26 which were deprotected using 1:1 TFA/CH₂Cl₂, affording the free amines 27 and 28. These were in turn reacted with 2,4-difluorobenzenesulfonyl chloride in pyridine to provide benzenesulfonamide targets 3 and 4. For the remaining compounds of Table 1 (5−9), N-(5-bromopyridin-3-yl)-N-(ethoxymethyl)-2,4-difluorobenzenesulfonamide[16] was converted to the corresponding boronate using bis(pinacolato)-diboron under Pd-catalyzed conditions and reacted directly with the remaining iodides 20−24 in a series of Suzuki reactions. This gave the crude ethoxymethyl-protected intermediates which were collected by filtration and deprotected under acidic conditions to furnish final products 5-9.

For Scheme 2, dihydropyrrolo[3,4-b]pyridinones 29−31 were prepared using similar chemistry to that employed above. 3-Bromo-6-methyl-5,6-dihydro-7H-pyrrolo[3,4-b]pyridin-7-one (A), 3-bromo-5,6-dihydro-7H-pyrrolo[3,4-b]pyridin-7-one (B), and 3-bromo-6,7-dihydro-5H-pyrrolo[3,4-b]pyridin-5-one (C) are all commercially available and were reacted with 2-thiopheneboronic acid and iodinated as previously described[16] to give the required iodides 29−31. The sulfonamide halves of the target molecules were assembled through reaction of commercial sulfonyl chlorides and substituted 3-amino-5-bromopyridines, followed by protection of the resulting sulphonamide nitrogen under standard conditions with either Cbz or ethoxymethyl to give intermediates 32−37. In the absence of a protecting group the subsequent Suzuki step
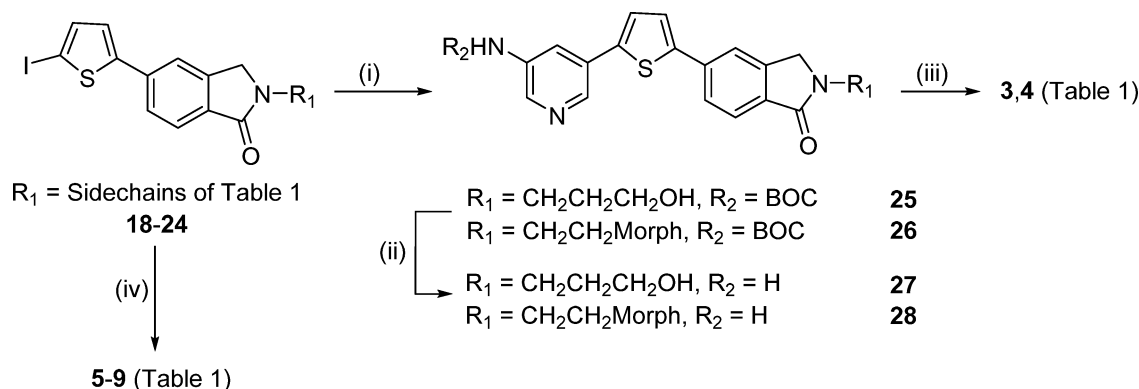
Table 2. N-Containing Isoindolinones
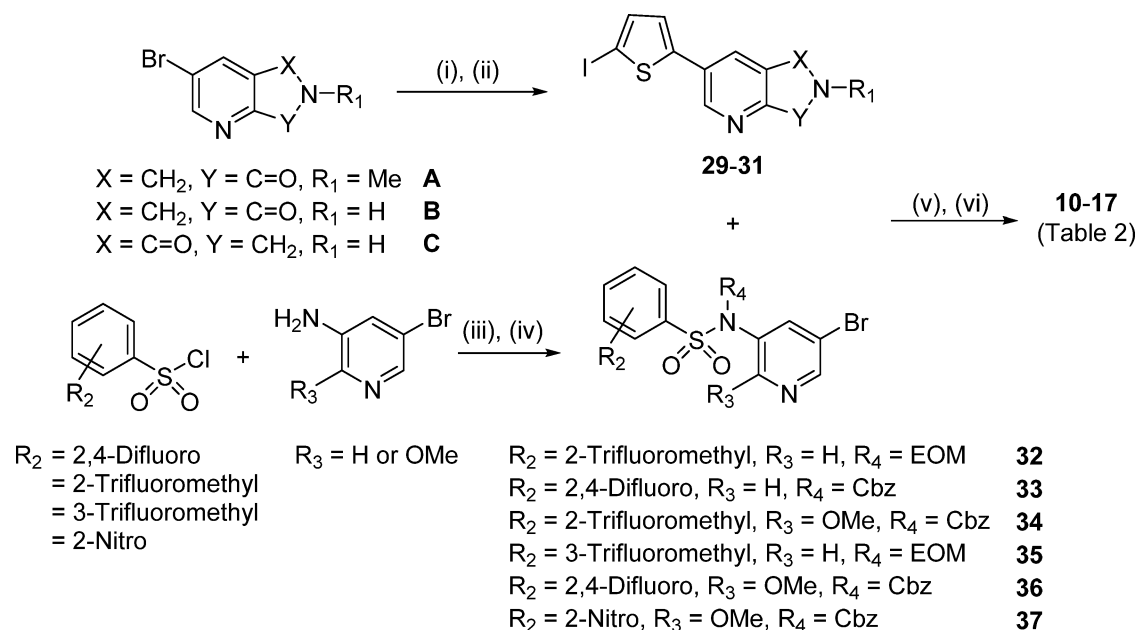

compd	R₁	R₂	R₃	inhibition of Jurkat lysis, IC₅₀ (μM)[a]	inhibition of KHYG1 NK, IC₅₀ (μM)[b]	KHYG1 viability (% at 10 μM)[c]
2[d]	2-NO₂	H		6.65	0.50	98.7 ± 1.5
10	2-CF₃	H	A	1.38	3.30	100
11	2,4-diF	H	B	5.73		49.0 ± 6.3
12	2-CF₃	OMe	A	0.78	2.21	95.8 ± 4.0
13	3-CF₃	H	A	>20	3.40	97.8 ± 1.8
14	2,4-diF	H	A	4.30	7.50	99.6 ± 0.2
15	2,4-diF	H	C	>20	6.80	100
16	2,4-diF	OMe	A	3.34	4.43	90.6 ± 5.0
17	2-NO₂	OMe	A	2.30	1.60	95.8 ± 4.0

[a]Testing was carried out over a range of concentrations, with the IC₅₀ being equal to the concentration at which 50% inhibition of the lysis of Jurkat cells by purified recombinant perforin was observed, as measured by ^{51}Cr release. Values are the average of at least three independent IC₅₀ determinations. [b]Testing was carried out over a range of concentrations, with the IC₅₀ being equal to the concentration at which 50% inhibition of the lysis of K562 target cells was observed when co-incubated with KHYG1 human NK cells, as measured by ^{51}Cr release. Values are the average of at least three independent IC₅₀ determinations. [c]Viability of KHYG1 NK cells after 24 h by Trypan blue exclusion assay. All results are the average of at least three separate determinations ± SEM. [d]Data from ref 17.

Scheme 1[a]

R1 = Sidechains of Table 1
18-24

R1 = CH2CH2CH2OH, R2 = BOC **25**
R1 = CH2CH2Morph, R2 = BOC **26**

R1 = CH2CH2CH2OH, R2 = H **27**
R1 = CH2CH2Morph, R2 = H **28**

5-9 (Table 1)

[a]Reagents and conditions: (i) *tert*-butyl (5-(4,4,5,5-tetramethyl-1,3,2-dioxaborolan-2-yl)pyridin-3-yl)carbamate, **18** or **19**, Pd(dppf)Cl₂, EtOH/toluene, 2 M Na₂CO₃, reflux; (ii) TFA, CH₂Cl₂ (1:1), rt; (iii) 2,4-difluorobenzenesulfonyl chloride, pyridine, 0−45 °C; (iv) (a) *N*-(5-bromopyridin-3-yl)-*N*-(ethoxymethyl)-2,4-difluorobenzenesulfonamide, bis(pinacolato)diboron, KOAc, Pd(dppf)Cl₂, DMSO, 90 °C; (b) **20−24**, crude *N*-(ethoxymethyl)-2,4-difluoro-*N*-(5-(4,4,5,5-tetramethyl-1,3,2-dioxaborolan-2-yl)pyridin-3-yl)benzenesulfonamide, Pd(dppf)Cl₂, EtOH/toluene, 2 M Na₂CO₃, reflux; (c) 3 M HCl, 1,4-dioxane (1:1), reflux.

Scheme 2[a]

X = CH2, Y = C=O, R1 = Me **A**
X = CH2, Y = C=O, R1 = H **B**
X = C=O, Y = CH2, R1 = H **C**

29-31

+

10-17
(Table 2)

R2 = 2,4-Difluoro
  = 2-Trifluoromethyl
  = 3-Trifluoromethyl
  = 2-Nitro

R3 = H or OMe

R2 = 2-Trifluoromethyl, R3 = H, R4 = EOM **32**
R2 = 2,4-Difluoro, R3 = H, R4 = Cbz **33**
R2 = 2-Trifluoromethyl, R3 = OMe, R4 = Cbz **34**
R2 = 3-Trifluoromethyl, R3 = H, R4 = EOM **35**
R2 = 2,4-Difluoro, R3 = OMe, R4 = Cbz **36**
R2 = 2-Nitro, R3 = OMe, R4 = Cbz **37**

[a]Reagents and conditions: (i) 2-thiopheneboronic acid, Pd(dppf)Cl₂, EtOH/toluene, 2 M Na₂CO₃, reflux; (ii) NIS, AcOH, CHCl₃, rt; (iii) pyridine, 0−45 °C; (iv) benzyl chloroformate, NaH, DMF, 0 °C or (chloromethoxy)ethane, NaH, DMF, rt; (v) (a) **32−37**, bis(pinacolato)diboron, KOAc, Pd(dppf)Cl₂, DMSO, 90 °C; (b) **29−31**, crude boronates, Pd(dppf)Cl₂, EtOH/toluene, 2 M Na₂CO₃, reflux, Cbz deprotected in situ (**32**, **34**, **36**, **37**); (vi) for ethoxymethyl deprotection (**33**, **35**) 3 M HCl, 1,4-dioxane (1:1), reflux.

either does not occur or proceeds in poor yield. Use of a benzyl carbamate was preferred (**33**, **34**, **36**, **37**), as the Cbz is deprotected in situ during the Suzuki step; however for a smaller number of examples, ethoxymethyl (**32**, **35**) was required for a successful reaction. Target compounds **10−17** were therefore obtained directly from the Suzuki step (**11**, **12**, **15**, **16**, **17**) or following deprotection of the *N*-ethoxymethyl using 1:1 3 M HCl/1,4-dioxane at reflux (**10**, **13**, **14**).

Inhibitory Activity of Benzenesulfonamides in Vitro. Our rationale for preparing N-substituted analogues **3−9** (Table 1) was based on a related series of *N*-hydroxyalkyl-substituted isoindolinones which were found to be potent inhibitors of recombinant perforin (≤1 μM).[14] We anticipated that structures of this type could potentially increase solubility

without being detrimental to activity. Unfortunately the previous SAR did not transfer to the current series as hydroxyalkyl derivatives **4** and **5** possessed only moderate activity while alcohol **3** and amines **6−10** were inactive at the concentrations tested (IC₅₀ > 20 μM). Each compound was also assessed for activity against perforin produced by an intact human NK cell line (KHYG1). Killer cells were treated with compound, labeled cells (K562 leukemia) were added, and the release of ⁵¹Cr label from the target cells was measured after incubation at 37 °C for 4 h. At a compound concentration of 20 μM, all examples (**3−9**) showed poor activity in this assay (data not shown).

We next investigated the effect of introducing a nitrogen atom to the isoindolinone benzene ring to give a series of

Table 3. Physicochemical Properties of Aza-isoindolinones

| compd | solubility (mg/mL)^{a,b} | cLogP^c | microsome stability (%)^{d,b} | | | stability in solution (%)^{e,b} | plasma protein binding (%)^{f,b} |
			mouse	rat	human		
2^g	0.67	1.83 ± 0.61	100	89	73	100	99.36
10	4.28	2.62 ± 0.71	86	36	56		
11	1.13	2.99 ± 0.83					
12	7.34	3.14 ± 0.76	91	50	63		
13	20.3	2.77 ± 0.71	88	84	46		
14	20.3	2.32 ± 0.78	100	100	80	100	99.94
15	3.77	2.72 ± 0.80	83	100	95	93	99.89
16	18.3	2.84 ± 0.82	100	100	75	100	99.91
17	4.81	1.99 ± 0.73	95	80	94	100	99.91

^{a}Solubility of the sodium salt in water at room temperature; conversion to salt as described in the Experimental Section. ^{b}See Supporting Information for further details of assay conditions. ^{c}cLogP calculated using ACD/PhysChem software version 12.5. ^{d}Percentage of parent compound (as sodium salt) remaining after exposure to mouse, rat, or human microsomes for 30 min. ^{e}Percentage of parent compound (as sodium salt) remaining after 24 h. at 20 °C as a solution in water. ^{f}Compound binding to mouse plasma was determined by equilibrium dialysis as described in the Experimental Section. ^{g}Data from ref 17.

dihydropyrrolo[3,4-b]pyridinones (Table 2). For the majority of compounds (**10−12**, **14**, **16**, **17**) this resulted in low-μM IC$_{50}$ values for inhibition of recombinant perforin-mediated lysis of labeled target cells, with analogue **12** clearly the best, possessing IC$_{50}$ = 0.78 μM. These results were anticipated based on the corresponding des-aza analogues;[17] however compounds **13** and **15** unexpectedly (and reproducibly) delivered poor activity in comparison to the rest of the series (both ~40% inhibition at 20 μM). Although 3-trifluoromethylbenzene **13** is the only example with a substituent at the *meta*-position of the benzene, and **15** the only example of a 6,7-dihydro-5H-pyrrolo[3,4-b]pyridin-5-one isomer, neither appear sufficiently distinct from remaining series members to account for this surprising loss of activity.

Compounds **10−17** were then tested for their ability to block whole KHYG1 NK cells as described above. Activity was excellent across the entire series, with IC$_{50}$ values ranging from 1.60 (**17**) to 7.50 μM (**14**). In contrast to their poor activity against recombinant perforin, compounds **13** and **15** also demonstrated potent inhibitory activity (IC$_{50}$ values of 3.40 and 6.80 μM, respectively). To confirm that the observed activity was due to blocking the action of perforin and not nonspecific toxicity toward the killer cell, viability was also measured 24 h after the NK cells were exposed to the target compounds. The KHYG1 NK cells showed good viability for almost all compounds, including examples **13** and **15**, showing that while their activity against recombinant perforin was relatively poor, the observed activity against NK cells is not due to death of the effector cells. The only exception in the series was 5,6-dihydro-7H-pyrrolo[3,4-b]pyridin-7-one **11**, which showed significant toxicity and was therefore eliminated from further consideration. Given their encouraging activity against whole NK cells, all remaining compounds of Table 2 were progressed to physicochemical and pharmacokinetic profiling studies. This was on the basis that the KHYG1 assay is a more physiologically relevant model than direct lysis with recombinant protein, as perforin is delivered into a synapse formed between the killer and target cell where it facilitates entry of granzymes (serine proteases), which in turn trigger apoptotic (rather than lytic) cell death.

Physicochemical Properties and in Vivo Pharmacokinetics of Selected Compounds. In the design of this dihydropyrrolo[3,4-b]pyridinone-based series, our primary objectives were to improve solubility and reduce cLogP. The solubilities of the compounds (as the sodium salts) were determined in water and ranged from 1.13 to 20.3 mg/mL (Table 3).

Interestingly, while for the *N*-methyl analogues **10**, **13**, and **14** the gain in solubility was substantial (approximately 20- to 50-fold over the corresponding isoindolinones which were 0.09, 0.57, and 1.08 mg/mL respectively[17]), the reverse was true for the two *N*H examples **11** and **15** where a 3- to 9-fold *loss* of solubility was observed (1.13 and 3.77 mg/mL for **11** and **15** compared to the isoindolinones 10.6 and 12.9 mg/mL [17]). As expected, introduction of a nitrogen to the isoindolinone benzene ring resulted in a drop in cLogP for all examples where pairs were available for comparison, from 2.70−3.48 for the des-aza compounds[17] to 2.32−2.99 for the corresponding dihydropyrrolo[3,4-b]pyridinones.

Next, the stability of the target compounds was examined more closely. 5,6-Dihydro-7H-pyrrolo[3,4-b]pyridin-7-one **11** was excluded from this analysis due to NK cell toxicity and relative insolubility. All remaining analogues were exposed to mouse, rat, or human liver microsomes, and then the percentage of parent remaining was determined after 30 min. Stability in the presence of mouse microsomes was excellent across the series; this is required given our in vivo efficacy model is in this species. Compounds **10**, **12**, and **13**, however, were less stable in the presence of human microsomes (and also rat in the cases of **10** and **12**) and were therefore not considered for further assessment. This left preferred examples **14−17**, all of which demonstrated good stability in water after 24 h at 20 °C (93−100%) and were Ames negative (data not shown). Plasma protein binding was determined for **2** and **14−17** and was extremely high, most likely due to the relatively acidic sulfonamide *N*H interacting with basic plasma proteins.

Plasma PK parameters were determined in male C57BL/6 mice for optimized compounds **14−17** (Table 4). Blood samples were collected at 5−8 time points after dosing in a solution of 20% hydroxypropyl-β-cyclodextrin (at 90, 150, 90, and 75 mg/kg, respectively) by intraperitoneal (ip) injection. Each analyte of interest was then quantitated using a validated LC−MS/MS method which included use of an internal standard.

Analogue **16** possessed the longest half-life (18.9 h), more than twice the length of either **14** or **15** (6.8 and 5.5 h, respectively) and far superior to **17** which was a disappointing 1.6 h. C$_{max}$ was similar for both **15** and **16** (1316 and 1310

Table 4. In Vivo Pharmacokinetics of Selected Compounds[a]

compd	dose[b] (mg/kg)	$T_{1/2}$ (h)	C_{max} (μmol/L)	$AUC_{0-\infty}$ ((μmol/L)·h)
14	90	6.8	860	10377
15	150	5.5	1316	7667
16	90	18.9	1310	42475
17	75	1.6	637	2237

[a]Pharmacokinetic parameters derived from the plasma-concentration−time profiles for each compound following the indicated ip dose. Results were processed using a noncompartment model approach using Phoenix WinNonlin 6.2 (Pharsight Corporation, St. Louis, MO). The derived parameters are maximum plasma concentration (C_{max}), the area under the curve (AUC), and plasma half-life ($T_{1/2}$). [b]The indicated dose was calculated as 75% of the predetermined maximum tolerated dose.

μmol/L, respectively) but with a significantly longer half-life; the total area under the curve was much greater for **16** compared to **15**. To determine if the plasma drug concentrations of the lead compounds were likely to be sufficient to see a therapeutic effect in spite of the high plasma protein binding, we compared the unbound plasma drug concentrations of **14** and **16** to the unbound in vitro perforin inhibition of these compounds. The unbound plasma drug concentrations were calculated by multiplying total plasma concentrations by the unbound fraction in plasma (1 − fraction plasma protein bound, Table 3) and were compared to the unbound in vitro IC_{50} values (3.42 μM, **14**; 1.13 μM, **16**), which were calculated as the IC_{50} in the KHYG1 assay (Table 2) multiplied by the unbound fraction in KHYG1 cell media (0.456, **14**; 0.255, **16**). At a dose of 90 mg/kg in male C57BL/6 mice, the unbound plasma concentrations of **16** exceeded the unbound IC_{50} for approximately 5−6 h after dosing; however for **14**, the unbound plasma concentrations did not reach the unbound IC_{50} (Figure 2). Overall, **16** clearly possessed the best balance of properties and was therefore selected for progression into our in vivo efficacy model.

In Vivo Efficacy of Candidate Compound 16 in a Mouse Model of Bone Marrow Transplant. Compound **16** was tested for efficacy in a short-term assay (24 h) of perforin-dependent NK cell-mediated graft rejection utilizing B6 perforin knockout recipients ($pfp^{-/-}$) as controls (Figure 3). This involved B6 mice receiving both allogeneic MHC-mismatched BALB/c stem cells and syngeneic MHC-matched B6 stem cells by bone marrow transplantation and perforin-dependent NK cell killing quantified by in vivo cytotoxicity

assays. Candidate **16** demonstrated a 66% reduction of perforin activity, resulting in preservation of transplanted mismatched target cells. Importantly we also showed that the compound was well tolerated, adequately soluble and that we had largely overcome the problems that had afflicted early analogues and precluded further development.

CONCLUSIONS

By utilizing a detailed structure−activity relationship that we had previously established for this class of benzenesulfonamide perforin inhibitors,[16,17] a focused set of new analogues was designed and prepared to optimize physicochemical and pharmacokinetic properties for in vivo studies. While our attempts to modulate cLogP and solubility via substitution on the isoindolinone nitrogen (**3−9**) were not successful, introduction of a nitrogen to the isoindolinone benzene ring was highly effective, resulting in the potent and soluble inhibitors **10** and **12−17**. Following further stability studies, this list was narrowed to four preferred compounds (**14−17**) for the measurement of in vivo pharmacokinetic parameters using ip dosing. All three were an improvement on our previous lead **2**, showing improved C_{max} and AUC and in the case of **16** a significantly enhanced half-life. Candidate **16** was consequently tested for its ability to preserve transferred MHC-mismatched cells in a short-term mouse model of bone marrow stem cell transplantation. In comparison to a perforin knockout recipient (representing 100% perforin "inhibition"), a 66% reduction in perforin activity was observed, as measured by survival of the transferred allogeneic cells. This result represents the first reported proof of principle that it is possible to inhibit perforin activity in vivo as a means of preserving bone marrow stem cell transplants. This approach could therefore be a viable method of preventing stem cell transplant rejection in patients where a perfect match is not available. We now plan to use these data to inform longer term mouse studies where bone marrow cells will be transplanted into lethally irradiated wild-type recipients, to more closely replicate established clinical conditions.

EXPERIMENTAL SECTION

Medicinal Chemistry. Analyses were performed by the Microchemical Laboratory, University of Otago, Dunedin, NZ. Melting points were determined using an Electrothermal model 9200 and are as read. NMR spectra were measured on a Bruker Advance 400 MHz spectrometer and referenced to Me$_4$Si. Mass spectra were recorded on either a Varian VG 7070 spectrometer at nominal 5000 resolution or a
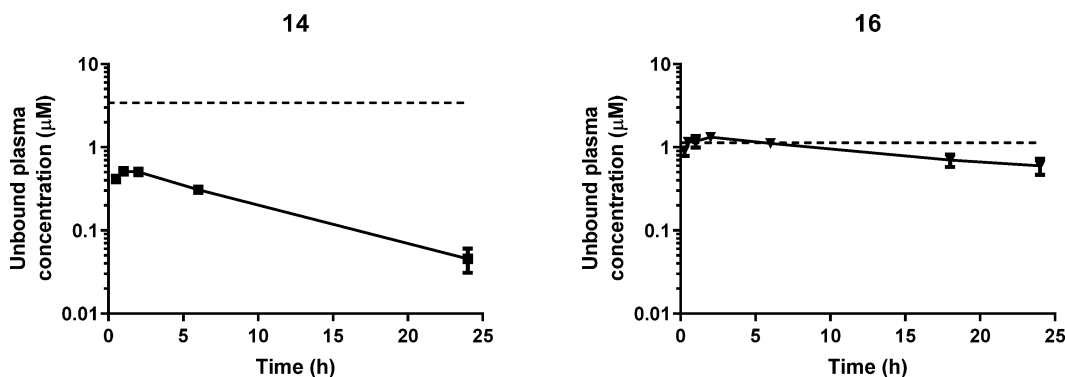

Figure 2. Unbound plasma concentrations of **14** and **16** relative to unbound IC_{50} in KHYG1 cells (dotted line). Symbols are the mean $\pm$ SEM of three mice.
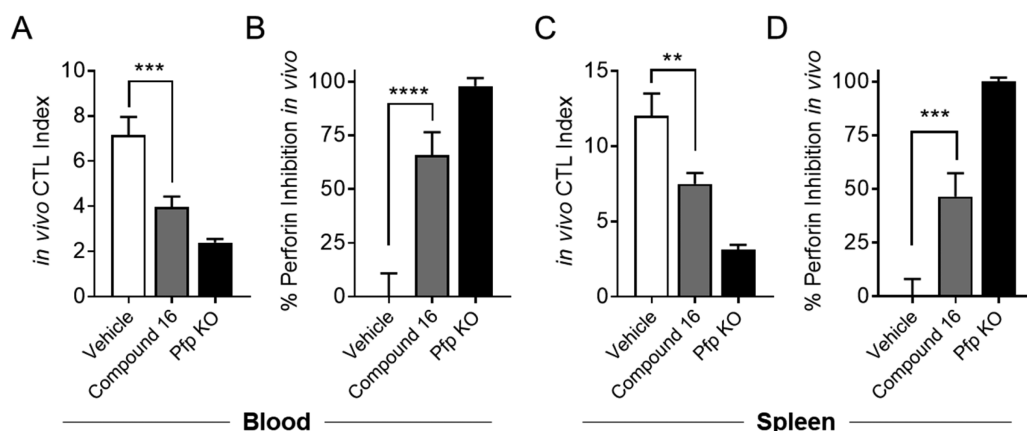
Figure 3. In vivo cytotoxic T lymphocyte (CTL) indices (A, C) and percentage perforin inhibition (B, D) in peripheral blood and spleen, derived from allogeneic bone marrow survival 24 h after transplant into wild type C57Bl/6 recipients (treated with either vehicle or 125 mg/kg compound **16**) or perforin deficient C57Bl/6 recipients (Pfp KO). Data represent pooled data from two independent experiments (vehicle = 10 mice/group, compound **16** = 10 mice/group, Pfp KO = 8 mice/group) and are shown as the mean ± SEM, and statistical comparison was performed by one-way ANOVA (**$p < 0.01$, ***$p < 0.001$, ****$p < 0.0001$).

Finnigan MAT 900Q spectrometer. All final compound purities were determined to be >95% by HPLC on an Alltech Alltima C18 column (3.2 mm × 150 mm, 5 μm) eluting with 5−80% MeCN/45 mM NH$_4$HCO$_3$.

Representative general procedures are given below. Full experimental information for all intermediates and final products is given in the Supporting Information.

General Procedure A: 2,4-Difluoro-N-(5-(5-(2-(3-hydroxypropyl)-1-oxoisoindolin-5-yl)thiophen-2-yl)pyridin-3-yl)-benzenesulfonamide (3) (Scheme 1). To 5-(5-(5-aminopyridin-3-yl)thiophen-2-yl)-2-(3-hydroxypropyl)isoindolin-1-one (**27**) (145 mg, 0.39 mmol) in dry pyridine (12 mL) under N$_2$ at room temperature was added dropwise 2,4-difluorobenzenesulfonyl chloride (247 mg, 1.16 mmol) over 5 min. The suspension was heated to 45 °C under N$_2$ for 4 h, at which point another portion of 2,4-difluorobenzenesulfonyl chloride (247 mg, 1.16 mmol) was added dropwise to complete the reaction. The mixture was left to stir at 45 °C under N$_2$ for 16 h, and then the solvent was removed under reduced pressure. The resulting residue was suspended in acetone (10 mL), 1 M HCl (20 mL) added, and the entire mixture stirred for 10 min. The solid was then collected by filtration, washed well with 1 M HCl and water, dried, and purified by chromatography as described below.

In cases where the bis-sulfonamide was also formed, a second step was introduced where the crude product above was treated with a 1:1 mixture of 1,4-dioxane and 2 M NaOH. The crude sulfonamide resulting from subsequent acidification of the reaction mixture was isolated by filtration, washed well with water, and dried. Purification was carried out by flash column chromatography (2% MeOH/CH$_2$Cl$_2$ as eluant) to give **3** as a pale pink solid (23 mg, 11%), mp (MeOH/CH$_2$Cl$_2$) 239−241 °C. ^{1}H NMR [400 MHz, (CD$_3$)$_2$SO] δ 11.15 (br s, 1 H), 8.69 (d, J = 1.8 Hz, 1 H), 8.25 (d, J = 2.4 Hz, 1 H), 7.97−8.04 (m, 1 H), 7.94 d, J = 0.7 Hz, 1 H), 7.84 (dd, J = 8.0, 1.5 Hz, 1 H), 7.69−7.74 (m, 3 H), 7.65 (d, J = 3.9 Hz, 1 H), 7.53−7.60 (m, 1 H), 7.27−7.34 (m, 1 H), 4.50−4.56 (m, 3 H), 3.59 (t, J = 7.2 Hz, 2 H), 3.45 (q, J = 5.8 Hz, 2 H), 1.76 (pentet, J = 6.7 Hz, 2 H). LRMS (APCI$^+$) calcd for C$_{26}$H$_{22}$F$_2$N$_3$O$_4$S$_2$ 542 (MH$^+$), found 542. Anal. (C$_{26}$H$_{21}$F$_2$N$_3$O$_4$S$_2$) C, H, N.

2,4-Difluoro-N-(5-(5-(2-(2-morpholinoethyl)-1-oxoisoindolin-5-yl)thiophen-2-yl)pyridin-3-yl)benzenesulfonamide (4). 5-(5-(5-Aminopyridin-3-yl)thiophen-2-yl)-2-(2-morpholinoethyl)-isoindolin-1-one (**28**) was reacted with 2,4-difluorobenzenesulfonyl chloride according to general procedure A, and the resulting crude product was purified by flash column chromatography (0.1% NH$_4$OH in 5% MeOH/CH$_2$Cl$_2$ as eluant) to give **4** as an off-white solid (11%), mp (MeOH/CH$_2$Cl$_2$) 249−251 °C. ^{1}H NMR [400 MHz, (CD$_3$)$_2$SO] δ 11.11 (br s, 1 H), 8.65 (br s, 1 H), 8.23 (d, J = 2.3 Hz, 1

H), 7.94−8.04 (m, 2 H), 7.84 (dd, J = 8.0, 1.5 Hz, 1 H), 7.69−7.74 (m, 3 H), 7.64 (d, J = 3.8 Hz, 1 H), 7.50−7.58 (m, 1 H), 7.29 (td, J = 8.4, 2.1 Hz, 1 H), 4.61 (s, 2 H), 3.67 (t, J = 6.2 Hz, 2 H), 3.56 (t, J = 4.5 Hz, 4 H), 2.58 (t, J = 6.2 Hz, 2 H), 2.45 (br s, 4 H). LRMS (APCI$^+$) calcd for C$_{29}$H$_{27}$F$_2$N$_4$O$_4$S$_2$ 597 (MH$^+$), found 597. Anal. (C$_{29}$H$_{26}$F$_2$N$_4$O$_4$S$_2$) C, H, N.

General Procedure B: N-(5-(5-(2-(2,3-Dihydroxypropyl)-1-oxoisoindolin-5-yl)thiophen-2-yl)pyridin-3-yl)-2,4-difluorobenzenesulfonamide (5). N-(5-Bromopyridin-3-yl)-N-(ethoxymethyl)-2,4-difluorobenzenesulfonamide[16] (357 mg, 0.88 mmol), bis(pinacolato)diboron (244 mg, 0.96 mmol), KOAc (258 mg, 2.63 mmol), and Pd(dppf)Cl$_2$ (36 mg, 0.04 mmol) were weighed into a flask. DMSO (6 mL) was added and the entire mixture heated and stirred under N$_2$ for 4 h. Upon cooling, the reaction was diluted with CH$_2$Cl$_2$ (40 mL) and filtered through a pad of Celite, washing well with additional CH$_2$Cl$_2$. The filtrate and combined washings (∼100 mL) was washed with water (3 × 50 mL), brine (50 mL), dried (Na$_2$SO$_4$), and filtered. Removal of the solvent under reduced pressure gave the desired boronate as a black-brown oil which was filtered through a plug of silica gel (50% EtOAc/hexanes as eluant) to remove colored baseline impurities, then used directly in the next step.

General Procedure C. The above crude boronate (348 mg, 0.88 mmol) was reacted with 2-(2,3-dihydroxypropyl)-5-(5-iodothiophen-2-yl)isoindolin-1-one (**20**) (332 mg, 0.80 mmol) by dissolving both starting materials in a mixture of toluene (12 mL) and EtOH (6 mL), adding 2 M Na$_2$CO$_3$ (3 mL) and Pd(dppf)Cl$_2$ (36 mg, 0.04 mmol), and heating the entire mixture at reflux under N$_2$ for 2 h. Upon cooling, the mixture was diluted with water (100 mL) and extracted with CH$_2$Cl$_2$ (6 × 50 mL). The combined organic fractions were dried (Na$_2$SO$_4$), filtered, and concentrated to give a solution from which the protected product was precipitated as a white solid by slow addition of n-hexane. This intermediate was subjected to a one-pot deprotection by taking the solid up in a 1:1 solution of 3 M HCl and 1,4-dioxane and heating to reflux for 1 h. Upon cooling, **5** precipitated as a white solid which was collected by filtration and dried. No further purification was required (82 mg, 18%), mp (MeOH/CH$_2$Cl$_2$) 188−191 °C. ^{1}H NMR [400 MHz, (CD$_3$)$_2$SO] δ 11.19 (br s, 1 H), 8.71 (d, J = 2.0 Hz, 1 H), 8.27 (d, J = 2.4 Hz, 1 H), 7.98−8.05 (m, 1 H), 7.96 (br s, 1 H), 7.84 (dd, J = 7.9, 1.5 Hz, 1 H), 7.70−7.77 (m, 3 H), 7.67 (d, J = 3.8 Hz, 1 H), 7.58 (ddd, J = 10.1, 9.2, 2.4 Hz, 1 H), 7.32 (ddd, J = 8.3, 8.3, 2.0 Hz, 1 H), 4.56−4.71 (m, 4 H), 3.72−3.80 (m, 1 H), 3.68 (dd, J = 13.9, 3.8 Hz, 1 H), 3.30−3.47 (m, 3 H). HRMS (ESI$^+$) calcd for C$_{26}$H$_{22}$F$_2$N$_3$O$_5$S$_2$ 558.0964 (MH$^+$), found 558.0966.

N-(5-(5-(2-(2-(Dimethylamino)ethyl)-1-oxoisoindolin-5-yl)-thiophen-2-yl)pyridin-3-yl)-2,4-difluorobenzenesulfonamide (6). N-(5-Bromopyridin-3-yl)-N-(ethoxymethyl)-2,4-difluorobenzene-

sulfonamide[16] was converted to the corresponding boronate according to general procedure B, then reacted with 2-(2-(dimethylamino)ethyl)-5-(5-iodothiophen-2-yl)isoindolin-1-one (**21**) according to general procedure C. In this case the sodium salt of the title compound was obtained through the slow addition of 2 M NaOH to the deprotection mixture to precipitate the title product. This was collected by filtration and dried to give **6** as a pale yellow solid (64%), mp (MeOH/CH₂Cl₂) 236 °C (dec). ¹H NMR (400 MHz, MeOD) δ 8.20 (d, *J* = 2.0 Hz, 1 H), 8.08 (d, *J* = 2.4 Hz, 1 H), 7.94–8.02 (m, 1 H), 7.86 (br s, 1 H), 7.80 (dd, *J* = 8.0, 1.4 Hz, 1 H), 7.77 (dd, *J* = 8.0, 0.4 Hz, 1 H), 7.70 (t, *J* = 2.2 Hz, 1 H), 7.53 (d, *J* = 3.9 Hz, 1 H), 7.38 (d, *J* = 3.8 Hz, 1 H), 7.00–7.08 (m, 2 H), 4.59 (s, 2 H), 3.79 (t, *J* = 6.6 Hz, 2 H), 2.69 (t, *J* = 6.6 Hz, 2 H), 2.35 (s, 6 H). HRMS (ESI⁺) calcd for $C_{27}H_{25}F_2N_4O_3S_2$ 555.1331 (MH⁺), found 555.1363.

2,4-Difluoro-*N*-(5-(5-(1-oxo-2-(2-(pyrrolidin-1-yl)ethyl)-isoindolin-5-yl)thiophen-2-yl)pyridin-3-yl)benzene-sulfonamide (7). *N*-(5-Bromopyridin-3-yl)-*N*-(ethoxymethyl)-2,4-difluorobenzenesulfonamide[16] was converted to the corresponding boronate according to general procedure B, then reacted with 5-(5-iodothiophen-2-yl)-2-(2-(pyrrolidin-1-yl)ethyl)isoindolin-1-one (**22**) according to general procedure C. The sodium salt of the title compound was obtained through slow addition of 2 M NaOH to the deprotection mixture to precipitate **7** as a yellow solid which was collected by filtration and dried (42%), mp (MeOH/CH₂Cl₂) 217 °C (dec). ¹H NMR (400 MHz, MeOD) δ 8.15 (d, *J* = 2.0 Hz, 1 H), 8.07 (d, *J* = 2.4 Hz, 1 H), 7.94–8.02 (m, 1 H), 7.86 (br s, 1 H), 7.75–7.83 (m, 2 H), 7.68 (t, *J* = 2.2 Hz, 1 H), 7.53 (d, *J* = 3.8 Hz, 1 H), 7.38 (d, *J* = 3.8 Hz, 1 H), 6.99–7.06 (m, 2 H), 4.60 (s, 2 H), 3.80 (t, *J* = 6.7 Hz, 2 H), 2.84 (t, *J* = 6.7 Hz, 2 H), 2.62–2.72 (br m, 4 H), 1.77–1.88 (br m, 4 H). HRMS (ESI⁺) calcd for $C_{29}H_{27}F_2N_4O_3S_2$ 581.1487 (MH⁺), found 581.1520.

2,4-Difluoro-*N*-(5-(5-(1-oxo-2-(2-(piperidin-1-yl)ethyl)-isoindolin-5-yl)thiophen-2-yl)pyridin-3-yl)benzene-sulfonamide (8). *N*-(5-Bromopyridin-3-yl)-*N*-(ethoxymethyl)-2,4-difluorobenzenesulfonamide[16] was converted to the corresponding boronate according to general procedure B, then reacted with 5-(5-iodothiophen-2-yl)-2-(2-(piperidin-1-yl)ethyl)isoindolin-1-one (**23**) according to general procedure C. In this case preparative HPLC [Synergi Max RP prep column, mobile phase gradient composed of A = TFA/H₂O (pH = 2.56), B = 90% acetonitrile/10% H₂O, flow rate 12 mL/min] was required for purification to obtain **8** as a yellow solid (trifluoroacetate salt) (10%), mp (MeOH/CH₂Cl₂) 157–160 °C. ¹H NMR [400 MHz, (CD₃)₂SO] δ 11.16 (s, 1 H), 8.86 (br s, 1 H), 8.71 (d, *J* = 2.0 Hz, 1 H), 8.26 (d, *J* = 2.4 Hz, 1 H), 7.97–8.04 (m, 2 H), 7.88 (dd, *J* = 8.0, 1.5 Hz, 1 H) 7.74–7.79 (m, 2 H), 7.68 (d, *J* = 3.9 Hz, 1 H), 7.54–7.61 (m, 1 H), 7.28–7.35 (m, 1 H), 4.58 (s, 2 H), 3.93 (t, *J* = 3.9 Hz, 2 H), 3.57–3.66 (m, 2 H), 2.57–3.00 (m, 2 H), 1.80–1.90 (m, 2 H), 1.53–1.75 (m, 4 H), 1.34–1.46 (m, 2 H). HRMS (ESI⁺) calcd for $C_{30}H_{29}F_2N_4O_3S_2$ 595.1644 (MH⁺), found 595.1669.

2,4-Difluoro-*N*-(5-(5-(2-(2-(4-methylpiperazin-1-yl)ethyl)-1-oxoisoindolin-5-yl)thiophen-2-yl)pyridin-3-yl)benzene-sulfonamide (9). *N*-(5-Bromopyridin-3-yl)-*N*-(ethoxymethyl)-2,4-difluorobenzenesulfonamide[16] was converted to the corresponding boronate according to general procedure B, then reacted with 5-(5-iodothiophen-2-yl)-2-(2-(4-methylpiperazin-1-yl)ethyl)isoindolin-1-one (**24**) according to general procedure C. The sodium salt of the title compound was obtained through slow addition of 2 M NaOH to the deprotection mixture to precipitate **9** as a pale yellow solid which was collected by filtration and dried (38%), mp (MeOH/CH₂Cl₂) 202–205 °C. ¹H NMR [400 MHz, (CD₃)₂SO] δ 8.07 (d, *J* = 2.1 Hz, 1 H), 7.90–7.93 (m, 2 H), 7.78–7.88 (m, 2 H), 7.69 (d, *J* = 7.9 Hz, 1 H), 7.65 (d, *J* = 3.8 Hz, 1 H), 7.40–7.44 (m, 2 H), 7.19 (ddd, *J* = 9.7, 9.7, 2.5 Hz, 1 H), 7.04–7.11 (m, 1 H), 4.59 (s, 2 H), 3.63 (t, *J* = 6.2 Hz, 2 H), 2.54 (t, *J* = 6.2 Hz, 2 H), 2.36–2.46 (br s, 4 H), 2.20–2.36 (br s, 4 H), 2.13 (s, 3 H). HRMS (ESI⁺) calcd for $C_{30}H_{30}F_2N_5O_3S_2$ 610.1753 (MH⁺), found 610.1762.

N-(5-(5-(6-Methyl-7-oxo-6,7-dihydro-5H-pyrrolo[3,4-b]-pyridin-3-yl)thiophen-2-yl)pyridin-3-yl)-2-(trifluoromethyl)-benzenesulfonamide (10). *N*-(5-Bromopyridin-3-yl)-*N*-(ethoxy-

methyl)-2-(trifluoromethyl)benzenesulfonamide (**32**) was converted to the corresponding boronate according to general procedure B, then reacted with 3-(5-iodo-2,3-dihydrothiophen-2-yl)-6-methyl-5,6-dihydro-7H-pyrrolo[3,4-b]pyridin-7-one (**29**) according to general procedure C. In this case slow addition of 2 M NaOH to the deprotection mixture precipitated **10** as a pale yellow solid (sodium salt; 85%), mp (MeOH/CH₂Cl₂) 318–322 °C. ¹H NMR [400 MHz, (CD₃)₂SO] δ 9.04 (d, *J* = 2.1 Hz, 1 H), 8.29 (d, *J* = 2.1 Hz, 1 H), 8.13 (d, *J* = 7.8 Hz, 1 H), 8.07 (d, *J* = 2.1 Hz, 1 H), 7.91 (d, *J* = 2.4 Hz, 1 H), 7.74–7.79 (m, 2 H), 7.65 (br t, *J* = 7.7 Hz, 1 H), 7.54 (br t, *J* = 7.6 Hz, 1 H), 7.42 (d, *J* = 3.9 Hz, 1 H), 7.39 (t, *J* = 2.2 Hz, 1 H), 4.52 (s, 2 H), 3.12 (s, 3 H). Anal. ($C_{24}H_{16}F_3N_4NaO_3S_2 \cdot 2H_2O$) C, H, N.

2,4-Difluoro-*N*-(5-(5-(7-oxo-6,7-dihydro-5H-pyrrolo[3,4-b]-pyridin-3-yl)thiophen-2-yl)pyridin-3-yl)benzenesulfonamide (11). Benzyl (5-bromopyridin-3-yl)((2,4-difluorophenyl)sulfonyl)-carbamate (**33**) was converted to the corresponding boronate according to general procedure B, then reacted with 3-(5-iodothiophen-2-yl)-5,6-dihydro-7H-pyrrolo[3,4-b]pyridin-7-one (**30**) according to general procedure C during which the Cbz protecting group was also removed in situ. The resulting crude product was purified by flash column chromatography (5% MeOH/CH₂Cl₂ as eluant) to give the title compound **11** as a pale yellow solid (33%), mp (MeOH/CH₂Cl₂) > 300 °C. ¹H NMR [400 MHz, (CD₃)₂SO] δ 11.17 (s, 1 H), 9.11 (d, *J* = 2.1 Hz, 1 H), 9.00 (br s, 1 H), 8.72 (d, *J* = 2.0 Hz, 1 H), 8.35 (d, *J* = 2.1 Hz, 1 H), 8.28 (d, *J* = 2.4 Hz, 1 H), 7.98–8.05 (m, 1 H), 7.86 (d, *J* = 3.9 Hz, 1 H), 7.75 (t, *J* = 2.2 Hz, 1 H), 7.71 (d, *J* = 3.9 Hz, 1 H), 7.54–7.61 (m, 1 H), 7.28–7.34 (m, 1 H), 4.45 (s, 2 H). Anal. ($C_{22}H_{14}F_2N_4O_3S_2 \cdot 1.5H_2O$) C, H, N.

N-(2-Methoxy-5-(5-(6-methyl-7-oxo-6,7-dihydro-5H-pyrrolo[3,4-b]pyridin-3-yl)thiophen-2-yl)pyridin-3-yl)-2-(trifluoromethyl)benzenesulfonamide (12). Benzyl (5-bromo-2-methoxypyridin-3-yl)((2-(trifluoromethyl)phenyl)sulfonyl)carbamate (**34**) was converted to the corresponding boronate according to general procedure B, then reacted with 3-(5-iodothiophen-2-yl)-6-methyl-5,6-dihydro-7H-pyrrolo[3,4-b]pyridin-7-one (**29**) according to general procedure C during which the Cbz protecting group was also removed in situ. The resulting crude product was purified by flash column chromatography (2% MeOH/CH₂Cl₂ as eluant) to give a cream solid. This was converted to the corresponding sodium salt by suspension in EtOH, dropwise addition of aqueous 1 M NaOH (1 equiv), and dilution of the resulting solution with an equal volume of Et₂O resulting in crystallization of **12** as a pale yellow solid (sodium salt; 58%), mp (MeOH/CH₂Cl₂) 248 °C (dec). ¹H NMR [400 MHz, (CD₃)₂SO] δ 8.98 (d, *J* = 2.1 Hz, 1 H), 8.24 (d, *J* = 2.0 Hz, 1 H), 8.12 (d, *J* = 7.8 Hz, 1 H), 7.75 (d, *J* = 7.0 Hz, 1 H), 7.66–7.72 (m, 2 H), 7.63 (br t, *J* = 7.6 Hz, 1 H), 7.53 (br t, *J* = 7.5 Hz, 1 H), 7.32 (d, *J* = 2.3 Hz, 1 H), 7.12 (d, *J* = 3.9 Hz, 1 H), 4.51 (s, 2 H), 3.80 (s, 3 H), 3.11 (s, 3 H). Anal. ($C_{25}H_{18}F_3N_4NaO_4S_2 \cdot 2H_2O$) C, H, N.

N-(5-(5-(6-Methyl-7-oxo-6,7-dihydro-5H-pyrrolo[3,4-b]-pyridin-3-yl)thiophen-2-yl)pyridin-3-yl)-3-(trifluoromethyl)-benzenesulfonamide (13). *N*-(5-Bromopyridin-3-yl)-*N*-(ethoxymethyl)-3-(trifluoromethyl)benzenesulfonamide (**35**) was converted to the corresponding boronate according to general procedure B, then reacted with 3-(5-iodothiophen-2-yl)-6-methyl-5,6-dihydro-7H-pyrrolo[3,4-b]pyridin-7-one (**29**) according to general procedure C. The sodium salt of the title compound was obtained through the slow addition of 2 M NaOH to the deprotection mixture to give **13** as a pale yellow solid which was collected by filtration and dried (50%), mp (MeOH/CH₂Cl₂) > 300 °C. ¹H NMR [400 MHz, (CD₃)₂SO] δ 9.04 (d, *J* = 2.1 Hz, 1 H), 8.32 (d, *J* = 2.1 Hz, 1 H), 8.09 (d, *J* = 2.1 Hz, 1 H), 7.99–8.04 (m, 2 H), 7.92 (d, *J* = 2.4 Hz, 1 H), 7.78 (d, *J* = 3.8 Hz, 1 H), 7.74 (br d, *J* = 7.5 Hz, 1 H), 7.64 (br t, *J* = 8.0 Hz, 1 H), 7.47 (d, *J* = 3.9 Hz, 1 H), 7.42 (t, *J* = 2.2 Hz, 1 H), 4.53 (s, 2 H), 3.13 (s, 3 H). HRMS (ESI⁺) calcd for $C_{24}H_{18}F_3N_4O_3S_2$ 531.0767 (MH⁺), found 531.0795.

2,4-Difluoro-*N*-(5-(5-(6-methyl-7-oxo-6,7-dihydro-5H-pyrrolo[3,4-b]-pyridin-3-yl)thiophen-2-yl)pyridin-3-yl)-benzenesulfonamide (14). *N*-(5-Bromopyridin-3-yl)-*N*-(ethoxy-methyl)-2,4-difluorobenzenesulfonamide[16] was converted to the corresponding boronate according to general procedure B, then reacted with 3-(5-iodothiophen-2-yl)-6-methyl-5,6-dihydro-7H-

pyrrolo[3,4-*b*]pyridin-7-one (**29**) according to general procedure C. Slow addition of 2 M NaOH to the deprotection mixture precipitated **14** as a pale yellow solid (sodium salt; 58%), mp (MeOH/CH$_2$Cl$_2$) 295−299 °C. ^{1}H NMR [400 MHz, (CD$_3$)$_2$SO] δ 9.06 (d, J = 2.2 Hz, 1 H), 8.32 (d, J = 2.1 Hz, 1 H), 8.09 (d, J = 2.1 Hz, 1 H), 7.92 (d, J = 2.4 Hz, 1 H), 7.82−7.89 (m, 1 H), 7.78 (d, J = 3.8 Hz, 1 H), 7.47 (d, J = 3.8 Hz, 1 H), 7.43 (t, J = 2.3 Hz, 1 H), 7.19 (ddd, J = 9.7, 9.7, 2.5 Hz, 1 H), 7.05−7.11 (m, 1 H), 4.53 (s, 2 H), 3.12 (s, 3 H). Anal. (C$_{23}$H$_{15}$F$_2$N$_4$NaO$_3$S$_2$·1.5H$_2$O) C, H, N.

2,4-Difluoro-*N*-(5-(5-(5-oxo-6,7-dihydro-5*H*-pyrrolo[3,4-*b*]-pyridin-3-yl)thiophen-2-yl)pyridin-3-yl)benzenesulfonamide (15). Benzyl (5-bromopyridin-3-yl)((2,4-difluorophenyl)sulfonyl)-carbamate (**33**) was converted to the corresponding boronate according to general procedure B, then reacted with 3-(5-iodothiophen-2-yl)-6,7-dihydro-5*H*-pyrrolo[3,4-*b*]pyridin-5-one (**31**) according to general procedure C during which the Cbz protecting group was also removed in situ. The resulting crude product was purified by flash column chromatography (2% MeOH/CH$_2$Cl$_2$ as eluant) to give a cream solid. This was converted to the corresponding sodium salt by suspension in EtOH, dropwise addition of aqueous 1 M NaOH (1 equiv), and dilution of the resulting solution with an equal volume of Et$_2$O resulting in crystallization of **15** as a beige solid (53%), mp (MeOH/CH$_2$Cl$_2$) > 300 °C. ^{1}H NMR [400 MHz, (CD$_3$)$_2$SO] δ 9.10 (d, J = 2.2 Hz, 1 H), 8.87 (br s, 1 H), 8.29 (d, J = 2.2 Hz, 1 H), 8.08 (d, J = 2.0 Hz, 1 H), 7.91 (d, J = 2.4 Hz, 1 H), 7.82−7.90 (m, 1 H), 7.78 (d, J = 3.8 Hz, 1 H), 7.44 (d, J = 3.8 Hz, 1 H), 7.41 (t, J = 2.3 Hz, 1 H), 7.18 (ddd, J = 9.7, 9.7, 2.5 Hz, 1 H), 7.07 (ddd, J = 8.4, 8.4, 2.0 Hz, 1 H), 4.47 (s, 2 H). Anal. (C$_{22}$H$_{14}$F$_2$N$_4$O$_3$S$_2$) C, H, N.

2,4-Difluoro-*N*-(2-methoxy-5-(5-(6-methyl-7-oxo-6,7-dihy-dro-5*H*-pyrrolo[3,4-*b*]pyridin-3-yl)thiophen-2-yl)pyridin-3-yl)-benzenesulfonamide (16). Benzyl (5-bromo-2-methoxypyridin-3-yl)((2,4-difluorophenyl)sulfonyl)carbamate (**36**) was converted to the corresponding boronate according to general procedure B, then reacted with 3-(5-iodothiophen-2-yl)-6-methyl-5,6-dihydro-7*H*-pyrrolo[3,4-*b*]pyridin-7-one (**29**) according to general procedure C during which the Cbz protecting group was also removed in situ. The resulting crude product was purified by flash column chromatography (2% MeOH/CH$_2$Cl$_2$ as eluant) to give a pale yellow solid. This was converted to the corresponding sodium salt by suspension in EtOH, dropwise addition of aqueous 1 M NaOH (1 equiv), and dilution of the resulting solution with an equal volume of Et$_2$O which resulted in crystallization of **16** as a yellow solid (60%), mp (MeOH/CH$_2$Cl$_2$) 261−264 °C (dec). ^{1}H NMR [400 MHz, (CD$_3$)$_2$SO] δ 9.03 (d, J = 2.1 Hz, 1 H), 8.28 (d, J = 2.1 Hz, 1 H), 7.83−7.90 (m, 1 H), 7.73 (d, J = 3.8 Hz, 1 H), 7.70 (d, J = 2.3 Hz, 1 H), 7.44 (d, J = 2.3 Hz, 1 H), 7.24 (d, J = 3.8 Hz, 1 H), 7.19 (ddd, J = 9.7, 9.7, 2.5 Hz, 1 H), 7.09 (ddd, J = 8.4, 8.4, 2.2 Hz, 1 H), 4.52 (s, 2 H), 3.77 (s, 3 H), 3.12 (s, 3 H). Anal. (C$_{24}$H$_{17}$F$_2$N$_4$NaO$_4$S$_2$·H$_2$O) C, H, N.

N-(2-Methoxy-5-(5-(6-methyl-7-oxo-6,7-dihydro-5*H*-pyrrolo[3,4-*b*]pyridin-3-yl)thiophen-2-yl)pyridin-3-yl)-2-nitrobenzenesulfonamide (17). Benzyl (5-bromo-2-methoxypyr-idin-3-yl)((2-nitrophenyl)sulfonyl)carbamate (**37**) was converted to the corresponding boronate according to general procedure B, then reacted with 3-(5-iodothiophen-2-yl)-6-methyl-5,6-dihydro-7*H*-pyrrolo[3,4-*b*]pyridin-7-one (**29**) according to general procedure C during which the Cbz protecting group was also removed in situ. The resulting crude product was purified by flash column chromatography (2% MeOH/CH$_2$Cl$_2$ as eluant) to give a pale yellow solid. This was converted to the corresponding sodium salt by suspension in EtOH, dropwise addition of aqueous 1 M NaOH (1 equiv), and dilution of the resulting solution with an equal volume of Et$_2$O which resulted in crystallization of **17** as a yellow solid (26%), mp (MeOH/CH$_2$Cl$_2$) 261−264 °C (dec). ^{1}H NMR [400 MHz, (CD$_3$)$_2$SO] δ 9.02 (d, J = 2.1 Hz, 1 H), 8.26 (d, J = 2.1 Hz, 1 H), 7.88 (dd, J = 7.7, 1.5 Hz, 1 H), 7.72 (d, J = 3.9 Hz, 1 H), 7.69 (d, J = 2.3 Hz, 1 H), 7.49−7.63 (m, 3 H), 7.32 (d, J = 2.3 Hz, 1 H), 7.20 (d, J = 3.8 Hz, 1 H), 4.52 (s, 2 H), 3.79 (s, 3 H), 3.12 (s, 3 H). HRMS (ESI$^+$) calcd for C$_{24}$H$_{20}$N$_5$O$_6$S$_2$ 538.0850 (MH$^+$), found 538.0889.

Inhibition of Perforin-Mediated Lysis of Jurkat Cells. The ability of the compounds to inhibit the lysis of nucleated (Jurkat T lymphoma) cells in the presence of 0.1% BSA was measured by release of ^{51}Cr label. Jurkat target cells were labeled by incubation in medium with 100 μCi ^{51}Cr for 1 h. The cells were then washed three times to remove unincorporated isotope and resuspended at 1×10^5 cells per mL in RPMI buffer supplemented with 0.1% BSA. Each test compound was preincubated to concentrations of 20, 10, 5, 2.5, and 1.25 μM with recombinant perforin for 30 min with DMSO as a negative control. ^{51}Cr labeled Jurkat cells were then added, and cells were incubated at 37 °C for 4 h. The supernatant was collected and assessed for its radioactive content on a γ counter (Wallac Wizard 1470 automatic γ counter). Each data point was performed in triplicate, and an IC$_{50}$ was calculated from the range of concentrations described above. Compounds with an IC$_{50}$ < 1 μM were titrated down to lower concentrations in the same manner as above, to determine an accurate IC$_{50}$.

KHYG-1 Cytotoxicity Assay. KHYG-1 cells were washed and resuspended in RPMI + 0.1% BSA at 4×10^5 cells/mL, and an amount of 50 μL of KHYG-1 cells was dispensed to each well of a 96-well V-bottom plate. RPMI (50 μL) + 0.1% BSA or 10% (final concentration) of serum was added to each well. Then test compounds were added to KHYG-1 cells at various concentrations up to 20 μM and incubated at room temperature for 20 min. 1×10^6 K562 target cells were labeled with 75 μCi ^{51}Cr in 200 μL of RPMI for 90 min at 37 °C. Cells were washed as described above and resuspended in 5 mL of RPMI + 0.1% BSA. An amount of 50 μL of ^{51}Cr labeled K562 leukemia target cells was added to each well of the KHYG-1 plate (effector/target 2:1) and incubated at 37 °C for 4 h. ^{51}Cr release was assayed using a Skatron harvesting press and radioactivity estimated on a gamma counter (Wallac Wizard 1470 automatic γ counter). The percentage of specific cytotoxicity was calculated using the following formula:

$$\% \text{ specific lysis} = \frac{(\text{experimental release} - \text{spontaneous release})}{(\text{maximum release} - \text{spontaneous release})} \times 100$$

and expressed as the mean of triplicate assays ± standard error of the mean.

Toxicity to KHYG-1 NK Cells. The toxicity assay was carried out in exactly the same manner as the killing assay above, but instead of adding the labeled K562 target cells, 100 μL of RPMI 0.1% BSA was added. Cells were incubated for 4 h at 37 °C and then washed ×3 in RPMI + 0.1% BSA. Cells were then resuspended in 200 μL of complete medium and incubated for 18−24 h at 37 °C. Trypan blue was added to each well. Viable (clear) cells and total (clear + blue) cells were counted, and the percentage of viable cells was calculated compared to DMSO treated cell control (% viability).

Plasma Pharmacokinetics and Maximum Tolerated Dose Determinations. Pharmacokinetic studies were carried out in healthy CD-1 male mice ($n = 3$ at each time point) using intraperitoneal administration of **14−17** at the indicated doses (75% of a predetermined maximum tolerated dose) in 20% 2-hydroxypropyl-β-cyclodextrin (Sigma-Aldrich). Blood was collected by cardiac puncture at 15 min, 30 min, 1 h, 2 h, 6 h, 18 h, and 24 h postdose in ice-cold K2-EDTA tubes. Plasma samples were separated by centrifuging at 6000g for 5 min and stored at −80 °C until analysis. Frozen plasma was thawed on wet ice on the day of analysis, then the sample (10 μL) was transferred to a clean microcentrifuge tube and mixed with three volumes of ice-cold acetonitrile/methanol (3:1 v/v) to precipitate the plasma proteins. The tubes were centrifuged at 15 000g for 10 min to obtain the clear supernatant which was mixed with 0.01% formic acid−water (1:1) and concentration of the parent drug measured through injection of 10−20 μL into an LC−MS/MS (Agilent 6410 series triple quadrupole mass spectrometry detector system). A Zorbax SB-C18, 50 mm × 2.1 mm, 5 μm column was used at a 0.5 mL/min flow rate, eluting with a gradient of organic phase (A), acetonitrile in water (80:20 v/v) containing 0.01% formic acid and aqueous phase (B), water containing 0.01% formic acid. LC−

MS/MS analysis was carried out using multiple reaction monitoring. Parent drug was quantified against a standard curve 0−250 ng/mL in control mouse plasma, and plasma samples from 15 min , 30 min, and 1 h were diluted with control mouse plasma (1:20 for 15 min, 1:10 for 30 min, and 1 h samples) to fit within this range. The resultant concentration vs time data were fitted (using Phoenix WinNonlin 6.2; Pharsight Corporation, St. Louis, MO) to calculate pharmacokinetic parameters including half-life ($T_{1/2}$), maximum concentration (C_{max}), area under the curve ($AUC_{0-\infty}$).

The MTD was determined by single dose intraperitoneal administration through a classical dose escalation design in C57BL/6 mice and defined as a dose level that was tolerated by mice ($n = 2-3$ mice/group) with a body weight loss of <10% and no death or detectable sickness. Mice were observed for 4 days postdose. All animal experiments were approved by the Animal Ethics Committee of the University of Auckland.

In Vivo Efficacy Studies. Bone marrow was isolated from the long bones of Balb/c (H2-Dd, CD45.2$^+$) and B6.SJL-Ptprca$^\pm$ (H2-Db, CD45.1$^+$CD45.2$^+$) mice and mixed at a 1:1 ratio prior to intravenous injection (24×10^6 cells total) into wild type C57Bl/6 (H2-Db, CD45.2$^+$) or perforin deficient (H2-Db, CD45.2$^+$) recipients. WT mice were treated by intraperitoneal injection with either 200 μL of vehicle (20% hydroxypropyl-β-cyclodextrin) or 200 μL of compound **16** (125 mg/kg dissolved in vehicle) at 0 h (immediately prior to cell transfer) and 18 h after cell transfer. Mice were bled 24 h post-transfer prior to euthanasia and spleen collection. PBMC and splenocytes were prepared by mechanical disruption (spleen) and red cell lysis prior to surface staining for flow cytometry. Cells were stained with anti-CD45-fluorescein isothiocyanate and anti-CD45.2-phycoerythrin mAbs (BioLegend, San Diego, CA) to identify allogeneic donor cells (CD45.1$^+$), syngeneic donor cells (CD45.1$^+$CD45.2$^+$), and recipient cells (CD45.2$^+$). The cell viability dye 7-aminoactinomycin D and the erythrocyte marker anti-TER119-allophycocyanin were used to exclude dead cells and red blood cells, respectively. Samples were acquired with an LSR Fortessa (BD, Franklin Lakes, NJ) and analyzed using FlowJo version 9.4 software (BD). Allogeneic and syngeneic donor cells were identified and gated as described above, and CTL indices were calculated using the following formula:

$$CTL\ index = \frac{\%\ syngeneic\ (CD45.1^+CD45.2^+)\ donor\ cells}{\%\ allogeneic\ (CD45.1^+)\ donor\ cells}$$

To minimize experimental variation, percentage perforin inhibition was derived by normalization of the CTL indices within each experiment prior to pooling across experiments. The mean CTL index of perforin deficient mice was set to 100% inhibition and the mean CTL index of vehicle treated mice set to 0% inhibition. This normalization was then applied to all mice within the experiment. Statistical tests were performed in Prism version 7 (GraphPad, San Diego, CA) by one-way ANOVA with multiple comparisons made to the vehicle treated group and corrected using Dunnett's test. All animal experiments were approved by the Animal Ethics Committee of the QIMR Berghofer Medical Research Institute.

■ ASSOCIATED CONTENT

Ⓢ Supporting Information

The Supporting Information is available free of charge on the ACS Publications website at DOI: 10.1021/acs.jmedchem.9b00881.

> Experimental procedures for all intermediate compounds, elemental analysis results, HRMS and HPLC data for all final compounds, and additional experimental details for the solubility, stability, plasma protein, and media binding studies (PDF)

> Molecular formula strings with in vitro data (CSV)

■ AUTHOR INFORMATION

Corresponding Author
*Phone: +64 9 9236149. E-mail: j.spicer@auckland.ac.nz.

ORCID Ⓞ
Julie A. Spicer: 0000-0001-9506-2818
William A. Denny: 0000-0001-7997-1843

Notes
The authors declare no competing financial interest.

■ ABBREVIATIONS USED

CTL, cytotoxic T lymphocyte; NK, natural killer; HLA, human leukocyte antigen; RPMI, Roswell Park Memorial Institute; PBMC, peripheral blood mononuclear cell

■ REFERENCES

(1) Law, R. H. P.; Lukoyanova, N.; Voskoboinik, I.; Caradoc-Davies, T. T.; Baran, K.; Dunstone, M. A.; D'Angelo, M. E.; Orlova, E. V.; Coulibaly, F.; Verschoor, S.; Browne, K. A.; Ciccone, A.; Kuiper, M. J.; Bird, P. I.; Trapani, J. A.; Saibil, H. R.; Whisstock, J. C. The structural basis for membrane binding and pore formation by lymphocyte perforin. *Nature* **2010**, *468*, 447−451.

(2) de Saint-Basile, G.; Menasche, G.; Fischer, A. Molecular mechanisms of biogenesis and exocytosis of cytotoxic granules. *Nat. Rev. Immunol.* **2010**, *10*, 568−579.

(3) Voskoboinik, I.; Whisstock, J. C.; Trapani, J. A. Perforin and granzymes: function, dysfunction and human pathology. *Nat. Rev. Immunol.* **2015**, *15*, 388−400.

(4) Chaudhry, M. S.; Gilmour, K. C.; House, I. G.; Layton, M.; Panoskaltsis, N.; Sohal, M.; Trapani, J. A.; Voskoboinik, I. Missense mutations in the perforin (PRF1) gene as a cause of hereditary cancer predisposition. *OncoImmunology* **2016**, *5*, e1179415.

(5) Pearl-Yafe, M.; Kaminitz, A.; Yolcu, E. S.; Yaniv, I.; Stein, J.; Askenasy, N. Pancreatic islets under attack: cellular and molecular effectors. *Curr. Pharm. Des.* **2007**, *13*, 749−760.

(6) Thomas, H. E.; Trapani, J. A.; Kay, T. W. H. The role of perforin and granzymes in diabetes. *Cell Death Differ.* **2010**, *17*, 577−585.

(7) Voskoboinik, I.; Dunstone, M. A.; Baran, K.; Whisstock, J. C.; Trapani, J. A. Perforin: structure, function and role in human immunopathology. *Immun. Rev.* **2010**, *235*, 35−54.

(8) Kondo, Y.; Kobayashi, K.; Asabe, S.; Shiina, M.; Niitsuma, H.; Ueno, Y.; Kobayashi, T.; Shimosegawa, T. Vigorous response of cytotoxic T lymphocytes associated with systemic activation of CD8+ T lymphocytes in fulminant hepatitis B. *Liver Int.* **2004**, *24*, 561−567.

(9) Barry, M.; Bleackley, R. C. Cytotoxic T lymphocytes: all roads lead to death. *Nat. Rev. Immunol.* **2002**, *2*, 401−409.

(10) Veale, J. L.; Liang, L. W.; Zhang, Q.; Gjertson, D. W.; Du, Z.; Bloomquist, E. W.; Jia, J.; Qian, L.; Wilkinson, A. H.; Danovitch, G. M.; Pham, P. -T. T.; Rosenthal, J. T.; Lassman, C. R.; Braun, J.; Reed, E. F.; Gritsch, H. A. Non-invasive diagnosis of cellular and antibody-mediated rejection by perforin and granzyme B in renal allografts. *Hum. Immunol.* **2006**, *67*, 777−786.

(11) Choy, J. C.; Kerjner, A.; Wong, B. W.; McManus, B. M.; Granville, D. J. Perforin mediates endothelial cell death and resultant transplant vascular disease in cardiac allografts. *Am. J. Pathol.* **2004**, *165*, 127−133.

(12) Lopez, J. A.; Susanto, O.; Jenkins, M. R.; Lukoyanova, N.; Sutton, V. R.; Law, R. H. P.; Johnston, A.; Bird, C. H.; Bird, P. I.; Whisstock, J. C.; Trapani, J. A.; Saibil, H. R.; Voskoboinik, I. Perforin forms transient pores on the target cell plasma membrane to facilitate rapid access of granzymes during killer cell attack. *Blood* **2013**, *121*, 2659−2668.

(13) Leung, C.; Hodel, A. W.; Brennan, A. J.; Lukoyanova, N.; Tran, S.; House, C. M.; Kondos, S. C.; Whisstock, J. C.; Dunstone, M. A.; Trapani, J. A.; Voskoboinik, I.; Saibil, H. R.; Hoogenboom, B. W. Real-time visualization of perforin nanopore assembly. *Nat. Nanotechnol.* **2017**, *12*, 467−473.

(14) Spicer, J. A.; Lena, G.; Lyons, D. M.; Huttunen, K. M.; Miller, C. K.; O'Connor, P. D.; Bull, M.; Helsby, N. A.; Jamieson, S. M. F.; Denny, W. A.; Ciccone, A.; Browne, K. A.; Lopez, J. A.; Rudd-Schmidt, J.; Voskoboinik, I.; Trapani, J. A. Exploration of a series of 5-arylidene-2-thioxoimidazolidin-4-ones as inhibitors of the cytolytic protein perforin. *J. Med. Chem.* **2013**, *56*, 9542−9555.

(15) Miller, C. K.; Huttunen, K. M.; Denny, W. A.; Jaiswal, J. K.; Ciccone, A.; Browne, K. A.; Trapani, J. A.; Spicer, J. A. Diarylthiophenes as inhibitors of the pore-forming protein perforin. *Bioorg. Med. Chem. Lett.* **2016**, *26*, 355−360.

(16) Spicer, J. A.; Miller, C. K.; O'Connor, P. D.; Jose, J.; Huttunen, K. M.; Jaiswal, J. K.; Denny, W. A.; Akhlaghi, H.; Browne, K. A.; Trapani, J. A. Benzenesulphonamide inhibitors of the cytolytic protein perforin. *Bioorg. Med. Chem. Lett.* **2017**, *27*, 1050−1054.

(17) Spicer, J. A.; Miller, C. K.; O'Connor, P. D.; Jose, J.; Huttunen, K. M.; Jaiswal, J. K.; Denny, W. A.; Akhlaghi, H.; Browne, K. A.; Trapani, J. A. Substituted arylsulphonamides as inhibitors of perforin-mediated lysis. *Eur. J. Med. Chem.* **2017**, *137*, 139−155.

(18) Welz, M.; Eickhoff, S.; Abdullah, Z.; Trebicka, J.; Gartlan, K. H.; Spicer, J. A.; Demetris, A. J.; Akhlaghi, H.; Anton, M.; Manske, K.; Zehn, D.; Nieswandt, B.; Kurts, C.; Trapani, J. A.; Knolle, P.; Wohlleber, D.; Kastenmuller, W. Perforin inhibition protects from lethal endothelial damage during fulminant viral hepatitis. *Nat. Commun.* **2018**, *9*, 4805.

(19) Gluckman, E. Ten years of cord blood transplantation: from bench to bedside. *Br. J. Haematol.* **2009**, *147*, 192−199.

(20) Dahlberg, A.; Milano, F. Cord blood transplantation: rewind to fast forward. *Bone Marrow Transplant.* **2017**, *52*, 799−802.

(21) Servais, S.; Beguin, Y.; Baron, F. Emerging drugs for prevention of graft failure after allogeneic hematopoietic stem cell transplantation. *Expert Opin. Emerging Drugs* **2013**, *18*, 173−192.

(22) Martin, P. J.; Levy, R. B. Immune Rejection: The Immune Biology of Allogeneic Hematopoietic Stem Cell Transplantation (From Mice to Humans). In *Immune Biology of Allogeneic Hematopoietic Stem Cell Transplantation: Models in Discovery and Translation*; Socié, G., Blazar, B. R., Eds.; Elsevier: London, 2013; pp 83−122.

(23) Shizuru, J. A.; Bhattacharya, D.; Cavazzana-Calvo, M. The biology of allogeneic hematopoietic cell resistance. *Biol. Blood Marrow Transplant.* **2010**, *16*, S2−S7.

(24) Villard, J. The role of natural killer cells in human solid organ and tissue transplantation. *J. Innate Immun.* **2011**, *3*, 395−402.

(25) Westerhuis, G.; Maas, W. G. E.; Willemze, R.; Toes, R. E. M; Fibbe, W. E. Long-term mixed chimerism after immunologic conditioning and MHC-mismatched stem-cell transplantation is dependent on NK-cell tolerance. *Blood* **2005**, *106*, 2215−2220.

(26) Hamby, K.; Trexler, A.; Pearson, T. C.; Larsen, C. P.; Rigby, M. R.; Kean, L. S. NK cells rapidly reject allogeneic bone marrow in the spleen through a perforin- and Ly49D-dependent, but NKG2D-independent mechanism. *Am. J. Transplant.* **2007**, *7*, 1884−1896.

(27) Bogdandi, E. N.; Balogh, A.; Felgyinszki, N.; Szatmari, T.; Persa, E.; Hildebrandt, G.; Safrany, G.; Lumniczky, K. Effects of low-dose radiation on the immune system of mice after total-body irradiation. *Radiat. Res.* **2010**, *174*, 480−489.

(28) Trapani, J. A.; Smyth, M. J. Retroviral Vectors Encoding Recombinant Mouse Perforin, Its Expression and Therapeutic Uses Thereof. Patent WO2005083098A1, March 1, 2005.